1

Design and Development of an IoT-Based UV Meter and Dual-Axis Solar Tracker for Real-Time UV Index Monitoring Optimization

Dwi Agustian¹, Ilham Muthahhari², Valiant Yuvi Syahreza³, Anton Widodo⁴, Muchamad Rizqy Nugraha⁵, Edward Trihadi⁶

1.2.3,4.5.6Undergraduate Program in Applied of Instrumentation Meteorology, Climatology Geophysics (STMKG)

Article Info

Article history:

Received March 1, 2025 Revised March 6, 2025 Accepted March 7, 2025

Keywords:

UV Index Monitoring Internet of Things (IoT) Dual-Axis Solar Tracker

ABSTRACT

The ultraviolet (UV) radiation emitted by the sun has both positive and negative impacts on human life. Excessive exposure to UV rays can lead to various health issues, such as skin cancer and cataracts. Therefore, UV radiation monitoring becomes crucial, especially in the face of climate change, which may increase the intensity of UV radiation due to the depletion of the ozone layer. This study aims to design an Internet of Things (IoT)-based UV index monitoring system, equipped with a dual- axis solar tracker to optimize UV index measurements. The system utilizes the ESP32 microcontroller as the main processing unit, the UVM-30A sensor to detect UV radiation, and the DS3231 Real Time Clock (RTC) module for time synchronization. UV index data is displayed in real-time through a Liquid Crystal Display (LCD) screen and the Blynk platform for easy remote access. Test results show that the system performs well, with a low relative error compared to UV index data from the reference site uvindex.app. This system provides an innovative solution for efficient and real-time UV index monitoring, which can increase public awareness about the dangers of UV radiation.

This is an open access article under the <u>CC BY-SA</u> license.



Corresponden Author:

Dwi Agustan,

Undergraduate Program in Applied of Instrumentation Meteorology, Climatology Geophysics (STMKG) Tangerang City, Banten, Indonesia

Email: adwiagustian2003@gmail.com

1. INTRODUCTION

The sun is essentially a source of heat radiation that emits energy across a very broad wavelength range [1]. The relative intensity of UV radiation and visible light reaching the Earth's surface is greatly influenced by the atmosphere, which absorbs and scatters most of this radiation. At wavelengths below 320 nm, the intensity of UV radiation decreases drastically due to absorption by the stratospheric ozone layer [2]. Radiation with wavelengths below 288 nm almost does not reach the Earth's surface. Therefore, most of the known biological effects of solar radiation are related to the very short portion of the solar spectrum, which is less than 1.5% of the total solar energy reaching the Earth's surface.

Excessive exposure to ultraviolet (UV) radiation from the sun can cause serious health effects in humans, such as skin cancer, cataracts, and premature aging. Other harmful effects include various biological disorders, such as malignancies on the eyelids (for instance, basal cell carcinoma (BCC) and squamous cell carcinoma (SCC)), photokeratitis, pterygium, and cortical cataracts [3],[4].

As reported by the World Health Organization (WHO) in 2018, there are an estimated 2–3 million cases of non-melanoma skin cancer and 132,000 cases of melanoma each year worldwide, caused by excessive UV exposure [20]. Ultraviolet (UV) radiation is a form of electromagnetic radiation with wavelengths ranging from 100 to 400 nm, classified into three categories: UV-A (315–400 nm), UV-B (280–315 nm), and UV-C (100–280 nm [5].

Although UV radiation has negative health impacts, UV rays also have important benefits for life on Earth [6]. Since ancient times, UV rays have been believed to enhance the human immune system, strengthen bones and muscles, Journal of Computation Physics and Earth Science Vol. 5, No. 1, April 2025: 1-14

and be used in the treatment of skin diseases such as atopic dermatitis, psoriasis, localized scleroderma phototherapy, and vitiligo [7][8].

However, the dual nature of UV radiation, with both positive and negative effects, raises concerns about the health risks it poses. A study by Leal A.C. and colleagues noted an increase in health issues due to UV exposure, especially in tropical and subtropical regions [9].

In the 2015 UV Index meeting in Melbourne, Australia, it was agreed that raising awareness of the importance of protection from UV exposure, particularly for UV Index values of 3 and above, remains a significant public health issue. Although the UV Index (UVI) is not a standalone tool, its use can be more effective when combined with a more comprehensive sun protection strategy [10].

The Global UVI represents the intensity of UV radiation from the sun that reaches the Earth's surface, with values starting from zero and increasing. The higher the UVI value, the greater the potential for skin and eye damage, and the quicker the time required for damage to occur [11]. This index is designed to help the public understand the dangers of UV exposure and is widely used in public health campaigns to increase awareness about sun protection [12]. McKinlay and Diffey's research (1991) showed that the UVI can help the public take preventive actions based on predicted exposure levels [13]. Therefore, the UVI plays an important role in raising public awareness of UV exposure risks and reminding people to take necessary protective measures [14].

For these reasons, monitoring the UV index is crucial, especially during the current global climate change period, which affects the ozone layer and increases the intensity of UV radiation [12][15]. The use of an Internet of Things (IoT)-based UV index monitoring system offers the opportunity for real-time and continuous monitoring through UV sensors connected to cloud devices, enabling global data analysis and distribution, as well as providing innovative solutions for real-time data collection, which is very useful for environmental monitoring [16].

A solar tracker is a device that allows an LDR sensor to follow the movement of the sun to maximize energy absorption. There are two types: single-axis and dual-axis, with the dual-axis being more efficient because it can track the sun's position both vertically and horizontally [17][18]. Using the ESP32 as a controller in an IoT-based UV index reading system allows data to be collected and transmitted via Wi-Fi networks, enabling users to obtain real-time UV radiation data [19]. Several studies have shown that IoT-based environmental monitoring systems have successfully provided accurate data, helping relevant authorities make policies based on the monitoring results.

This study aims to design a system that provides real-time information related to the UV index, utilizing Internet of Things (IoT) technology to improve monitoring efficiency. This device integrates UV sensors with a dual-axis solar tracker system to optimize measurements by following the sun's movement, thus enabling more accurate UV index readings. The system is also equipped with the ability to send data directly to the Blynk platform, enabling remote monitoring that facilitates analysis and decision-making related to UV exposure.

2. METHODOLOGY

In this study, the author employed several stages, including system design, hardware design, and software design.

2.1 UV Index Threshold

Table 1 UV Radiation Exposure Categories

UV Index Range	Category	Color	
< 2	Low	Green	
3 - 5	Moderate	Yellow	
6 - 7	High	Orange	
8 - 10	Very High	Red	
11+	Extreme	Violet	

Table 1 shows the threshold values of the UV index used in the equipment system. These thresholds are divided into five categories to classify the UV index intensity: Low, Moderate, High, Very High, and Extreme. These categories help in clearly and structurally identifying the level of UV exposure.

2.2 System Design

The UV Index data processing results obtained from the designed device can be accessed in real-time through the Blynk platform. This allows users to monitor the device's status and the measured UV Index data. This enables efficient and practical monitoring without the need for direct physical interaction with the device.

The concept of this system will be explained in more detail through a block diagram and flowchart, illustrating the workflow and interaction between components in the system. The block diagram consists of three main interconnected and supporting sections: input, process, and output.

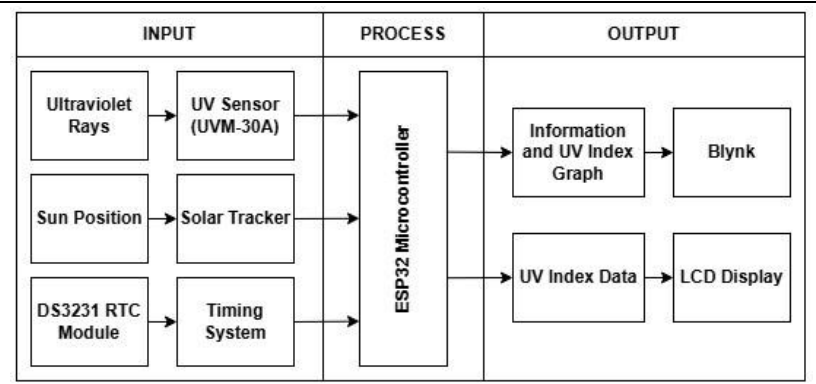


Fig. 1 Block Diagram System

2.2.1 Input

In this system, the inputs are the UV sensor, solar tracker, and timing system, which function to:

a. UV Sensor (UVM-30A)

The UV sensor is used to detect the UV index, which is the result of processing the output voltage generated by the sensor. The ESP32 microcontroller processes the voltage read from the sensor to calculate the UV index value according to the predetermined range. Each voltage value detected is processed into a UV index within the specified range.

b. Solar Tracker

The solar tracker consists of two SG90 servo motors and four LDR sensors. Each servo motor serves a different purpose: the vertical servo moves the panel vertically, while the horizontal servo moves the panel horizontally. The four LDR sensors are positioned in parallel at the top, bottom, left, and right, with barriers between each sensor to facilitate the detection of sunlight intensity. Each LDR sensor measures the intensity of light it receives, and based on the data from these sensors, the servo motors adjust the position of the solar panel to point toward the LDR sensor detecting the highest light intensity. This ensures that the UV sensor always faces the sun optimally.

c. Timing System

This device uses the DS3231 RTC module as the time management system, which functions to display real-time time information during operation. The module provides complete time information, including date, month, year, hour, minute, and second.

2.2.2 Process

The process in this system involves the ESP32 microcontroller, which functions to process data received from the input to produce the desired output. The ESP32 microcontroller processes data in the form of voltage output from the UV sensor, which is then converted into UV index values according to the predefined range. This data is displayed on an LCD screen and sent to the Blynk application in real-time.

Additionally, the ESP32 processes sunlight intensity data received from the LDR sensor, which then drives the servo motor to track the direction of sunlight.

2.2.3 Output

The output generated by this device consists of data displayed on an LCD and the Blynk application. The functions of each are as follows:

a. LCD 20x4

The LCD serves to display processed data from the ESP32, such as real-time UV index and time information. This LCD facilitates observers in monitoring the UV index during field observations, providing clear and easily accessible information directly on the device.

b. Blynk

Blynk functions to display UV index data, UV categories, reading time, and graphs on a web-based platform in real-time. The Blynk application can be accessed via laptops, computers, or mobile devices, offering convenience for users to monitor data remotely.

The system design is illustrated in the flow diagram shown in the image below:

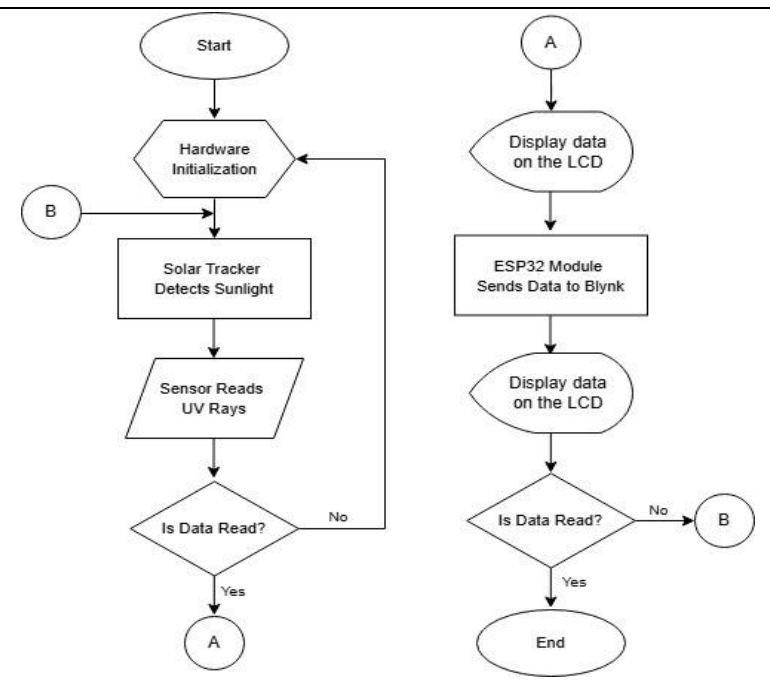


Fig. 2 System Flowchart

The flowchart above illustrates the workflow of an ESP32-based system for UV radiation monitoring using a solar tracker, UV sensor, and communication with Blynk. The following are the step-by-step explanations of the flowchart:

- The system is powered on and starts the program from the beginning to monitor and process data.
- Hardware components such as the solar tracker, sensors, RTC (Real-Time Clock), ESP32 module, and LCD
 are initialized to prepare them for use.
- The ESP32 module connects to a Wi-Fi network to enable data transmission to the Blynk monitoring application.
- The solar tracker begins monitoring the direction of sunlight to ensure proper alignment and determine the sun's position.
- The system reads data generated by the sensor and utilizes the RTC to record the timestamp of data collection.
- The system checks whether the sensor data has been correctly read. If successful, the process continues; if unsuccessful, the system retries data reading.
- Information obtained from the sensor is displayed on the LCD screen for easy readability.
- Data collected from the sensor is transmitted to the Blynk application, allowing users to monitor UV Index data from other devices, such as smartphones or laptops.
- The system checks if there is a command to shut down the device; if such a command exists, the system stops. Otherwise, the process returns to the sunlight detection step to continue the workflow cycle.
- End.

The visualization and explanation of the solar tracker flowchart are presented in the image below:

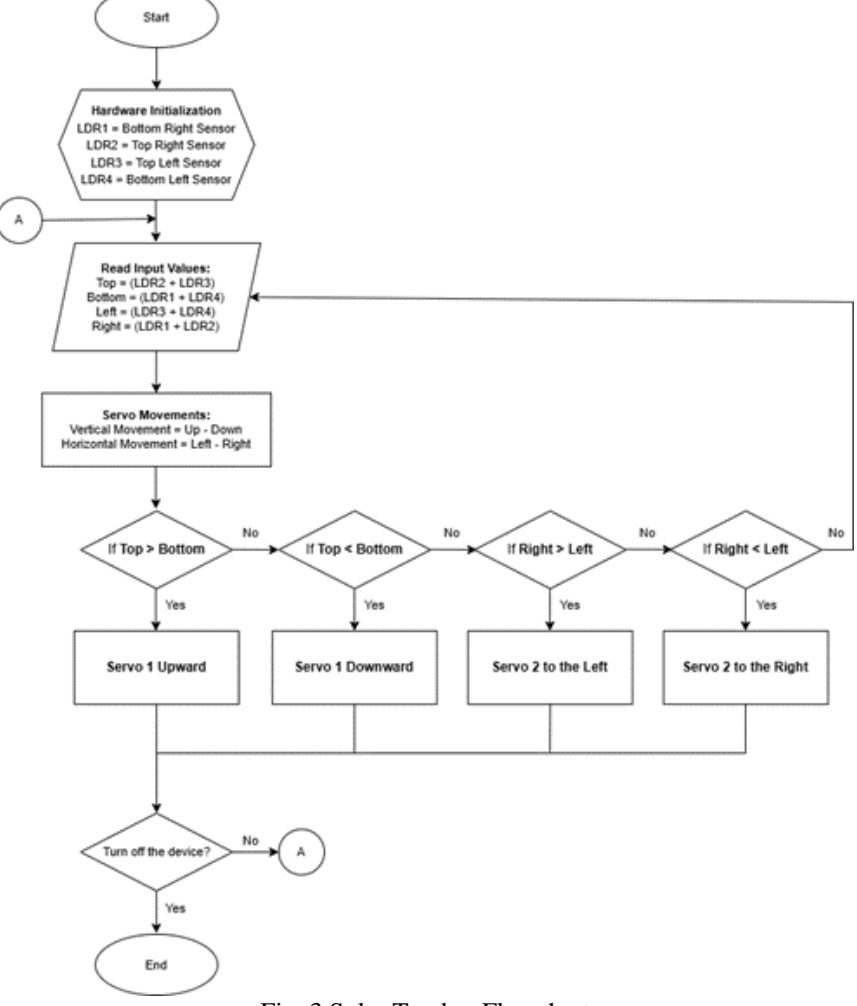


Fig. 3 Solar Tracker Flowchart

The flowchart above provides an overview of the workflow of the solar tracker, where a UV sensor is mounted on the tracker to ensure it remains perpendicular to the direction of incoming sunlight. The following is a detailed explanation of the solar tracker flowchart:

- The process begins by powering on the system.
- In the first step, the hardware is initialized by defining the positions of the LDR sensors:
 - LDR1 is placed in the bottom-right position.
 - LDR2 is placed in the top-right position.
 - LDR3 is placed in the top-left position.
 - LDR4 is placed in the bottom-left position.
- The system then reads the light intensity received by each LDR sensor. The obtained values are calculated as follows:
 - Top is calculated by summing the readings from LDR2 and LDR3.
 - Bottom is calculated by summing the readings from LDR1 and LDR4.
 - Left is calculated by summing the readings from LDR3 and LDR4.
 - Right is calculated by summing the readings from LDR1 and LDR2.
- Based on the sensor readings, the system determines the movements required by the servo motors. Vertical
 movement is calculated as the difference between the Top and Bottom values, while horizontal movement is
 calculated as the difference between the Right and Left values.
- If the Top value is higher than the Bottom value, the first servo motor moves upward. Conversely, if the Top value is less than the Bottom value, the first servo motor moves downward to adjust the vertical position.
- For horizontal movement, if the Right value is Higher than the Left value, the second servo motor moves to the left. However, if the Right value is less than the Left value, the second servo motor moves to the right.
- After the servo movement is executed, the system checks whether the device is turned off. If the device is
 powered off, the process ends and the system stops. If the device remains active, the process loops back to the
 sensor input reading step to adjust the servo movements according to the updated light intensity.
- The process concludes when the device is powered off, indicating that the system has completed its operation.

2.3 Hardware Design

Hardware design involves the comprehensive process of designing the physical structure of the system. The system circuit is created using Fritzing software, as illustrated in the image below:

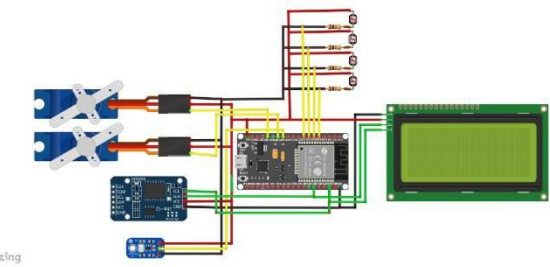


Fig. 4 Wiring Diagram

The image above depicts the wiring diagram of the UV meter and solar tracker system. The UV sensor, LDR, and servos are connected to the GPIO pins on the ESP32 microcontroller, while the LCD and DS3231 RTC module are connected to the SDA and SCL pins. The ESP32 microcontroller functions to process input data from the sensors and manage timing, displaying the data on a 20x4 LCD and transmitting it to the Blynk platform.

The overall hardware design planning includes a comprehensive overview of the device, starting with the solar tracker at the top, followed by a panel box that houses the microcontroller. The entire device design was created using Tinkercad, as shown in the image below.



Fig. 5 System Design

The solar tracker design planned in this study will function to track the direction both horizontally and vertically (dual axis), as shown in the image below.

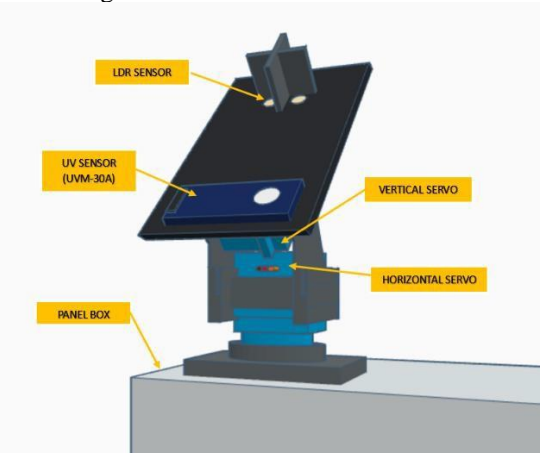


Fig. 6 Solar Tracker Design

The image shows that the solar tracker is placed in the upper left corner of the panel box, while all the sensors are connected with wires to the microcontroller inside the box. Two servos function as the horizontal and vertical servos, mounted on a bracket, allowing both servos to move left-right and up-down. On the black board, there are four LDRs separated by dividers, which serve to detect the direction of incoming sunlight. Meanwhile, the UV sensor is mounted beneath the LDRs so that it can be positioned perpendicular to the sunlight, ensuring optimal UV index readings.

2.4 Software Design

The UV index measurement data will then be displayed on Blynk. The displayed data includes the date and time of the reading, the UV index value, the UV index category, and a real-time graph of the UV index. The design of the display on Blynk, both on desktop and Android, is shown in the figure below.



Fig. 7 Blynk Desktop Diagram



Fig. 8 Blynk Android Display Design

2.5 Test and Calibration Plan

Device The testing plan involves comparison and calibration of the UV sensor, as well as adjusting the servo rotation angle to optimally track sunlight. The purpose of this calibration is to ensure that each sensor is suitable for use in the device. The UV index comparison is performed by comparing the UV index data obtained from the device with the reference data available on the uvindex.app website.



Fig. 9 Web Display of UV Index App

The data from the device is obtained through direct readings on the LCD display or remote monitoring via the Blynk platform. Once the data is collected, it is compared with the reference data, and the measurement differences are calculated. Subsequently, a linear regression graph will be created to evaluate whether the device provides results that are consistent with the reference data.

3. RESULT AND DISCUSSION

3.1 System Implementation

The implementation of the solar tracker along with the UV sensor that has been developed is shown in the image below:

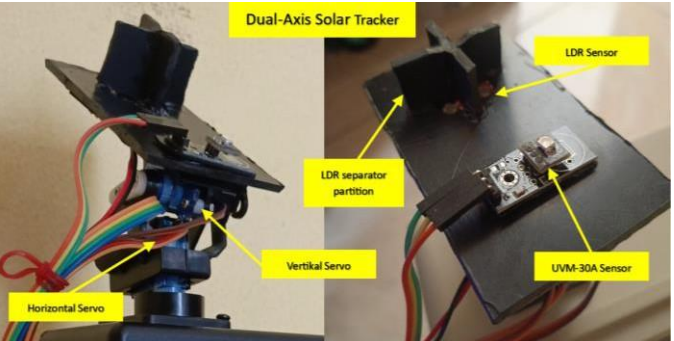


Fig. 10 Solar Tracker Implementation

The implementation of the panel box that has been constructed is shown in the image below:



Fig. 11 System Implementation

The overall implementation of the device is the integration of all system designs from this research. The panel box, which contains the ESP32 microcontroller, RTC, and LCD display, will be combined with the solar tracker into a single unit so that the device can function as intended. The overall appearance of the device, both inside and outside, is shown in the following images:



Fig. 12 Overall System Display

3.2 Testing and Calibration of the Device

The device testing was conducted in an open space on the second floor of the author's house, located in Tanah Tinggi Village, Tangerang City, Banten.

Journal of Computation Physics and Earth Science Vol. 5, No. 1, April 2025: 1-14

1. Solar Tracker

The solar tracker was tested under two conditions, indoors and outdoors. The indoor testing aimed to ensure that the solar tracker could properly detect the light source. Additionally, testing was conducted using a LED flash light to observe whether the solar tracker could accurately track the movement of the light direction from the LED flash light.

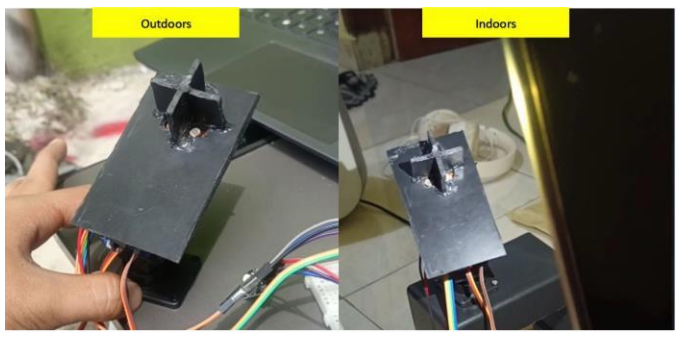


Fig. 13 Solar Tracker Testing

The test results show that the solar tracker functions well, both indoors and outdoors. This is demonstrated by its ability to accurately detect the direction of incoming rays.

2. DS3231 RTC Module

The testing of the DS3231 RTC module was carried out by comparing the date and time displayed on the RTC module through the serial monitor with the official time provided by BMKG, which can be accessed through the official BMKG website at https://jam.bmkg.go.id/Jam.BMKG.

```
Tanggal: 24/11/2024
Jam: 20:1:57
Tanggal: 24/11/2024
Jam: 20:1:59
Jam: 20:2:0
Jam: 20:2:0
Jam: 20:2:0
Jam: 20:2:0
Jam: 20:2:1
Jam: 20:2:3
Jam: 20:2:3
Jam: 20:2:3
Jam: 20:2:3
Jam: 20:2:4
Jam: 20:2:4
Jam: 20:2:5
Jam: 20:2:6
Jam: 20:2:7
Jam: 20:2:7
Jam: 20:2:9
Jam: 20:2:9
Jam: 20:2:9
Jam: 20:2:9
Jam: 20:2:10
```

Fig. 14 DS3231 Module Testing

3. UV Sensor (UVM-30A)

The UV sensor was tested by comparing the UV index values generated by the device with the UV index data available on the uvindex.app website. The UV index values on the device can be monitored manually through the serial monitor, the LCD display, or remotely using the Blynk platform.

```
6, HIGH, 11/12/2024, 11:32:24
6, HIGH, 11/12/2024, 11:32:25
5, MODERATE, 11/12/2024, 11:32:26
5, MODERATE, 11/12/2024, 11:32:27
5, MODERATE, 11/12/2024, 11:32:28
5, MODERATE, 11/12/2024, 11:32:29
6, HIGH, 11/12/2024, 11:32:31
6, HIGH, 11/12/2024, 11:32:32
```

Fig. 15 Serial Monitor Display



Fig. 16 LCD Display

If the reading values do not match the UV index data available on the uvindex.app website, calibration will be performed by checking the input and output voltages of the sensor and adjusting them to match the voltage range in the program.

```
JV Sensor Logic (Using GPIO 14)
sensorValue = analogRead(UV_SENSOR_PIN);
 at voltage = (sensorValue * (5.0 / 4095.0)) * 1000; // C
 (voltage < 50 || (voltage >= 50 && voltage <= 227)) {
UVIndex = "0";
else if (voltage > 227 && voltage <= 318) {
 else if (voltage > 318 && voltage <= 408) {
UVIndex
else if (voltage > 408 && voltage <= 503) {
UVIndex
 else if (voltage > 503 && voltage <= 606) {
else if (voltage > 606 && voltage <= 696) \{
UVIndex
else if (voltage > 696 && voltage <= 795) {
 lse if (voltage > 795 && voltage <= 881) {
UVIndex =
 else if (voltage > 881 && voltage <= 976) {
  lse if (voltage > 976 && voltage <= 1079) {
UVIndex = "9"; // Very high UV radiation
else if (voltage > 1079 && voltage <= 1170) {</pre>
UVIndex
           "10"; // Extreme UV radiation
 else if (voltage > 1170) {
```

Fig. 17 UV Sensor Output Range

Additionally, experiments were conducted by testing various angles of sunlight incidence on the UV sensor. The results showed that the most optimal UV sensor readings occurred when the sensor was placed perpendicular to the sunlight at a 90° angle. Therefore, the use of a solar tracker is necessary to ensure that the UV sensor remains in the optimal position for maximum UV readings.

Table 2 Solar Incident Angle Testing

Angle of Incidence of Sunlight	UV Index Reading
45°	5
60°	6
90°	7

After the UV meter was successfully constructed and calibrated, a comparison was made between the data generated by the UV meter and the reference from the Uvindex.app application under various times and weather conditions, namely clear and cloudy. This allowed for the verification of the accuracy and consistency of the UV readings between the two measurement methods. Data collection was conducted at nine observation times each day, from 08:00 to 16:00, with a one-hour interval. At each observation time, 15 samples were taken, the average value was computed to indicate the UV intensity for that specific hour. The correction was calculated as the difference between the UV meter value and the reference to evaluate the accuracy and consistency of the device. The results of this testing aim to assess the extent to which the UV meter can be used as a reliable device for monitoring UV intensity.

Table 3	UV	Sensor	Testing

Table 3 UV Sensor Testing									
No	Date, Time	Uvindex.app	UV meter	Weather	Correction				
1	28/11/2024, 08.00	3	3,2	Sunny	-0,2				
2	28/11/2024, 09.00	5	4,4	Sunny	0,6				
3	28/11/2024, 10.00	6	5,5	Sunny	0,5				
4	28/11/2024, 11.00	6	4,6	Cloudy	1,4				
5	28/11/2024, 12.00	7	6,7	Sunny	0,3				
6	28/11/2024, 13.00	6	5,4	Sunny	0,6				
7	28/11/2024, 14.00	6	6,1	Sunny	-0,1				
8	28/11/2024, 15.00	4	3,6	Sunny	0,4				
9	28/11/2024, 16.00	2	2,5	Cloudy	-0,5				
10	08/12/2024, 08.00	3	2,9	Sunny	0,1				
11	08/12/2024, 09.00	5	4,4	Sunny	0,6				
12	08/12/2024, 10.00	6	4,5	Sunny	1,5				
13	08/12/2024, 11.00	7	6,5	Cloudy	0,5				
14	08/12/2024, 12.00	7	6,6	Sunny	0,4				
15	08/12/2024, 13.00	6	4,3	Sunny	1,7				
16	08/12/2024, 14.00	6	5,5	Sunny	0,5				
17	08/12/2024, 15.00	4	3,6	Sunny	0,4				
18	08/12/2024, 16.00	2	1,9	Cloudy	0,1				
19	11/12/2024, 08.00	3	2,9	Sunny	0,1				
20	11/12/2024, 09.00	5	3,9	Sunny	1,1				
21	11/12/2024, 10.00	6	5,8	Sunny	0,2				
22	11/12/2024, 11.00	7	6,7	Cloudy	0,3				
23	11/12/2024, 12.00	8	7,4	Sunny	0,6				
24	11/12/2024, 13.00	7	5,9	Sunny	1,1				
25	11/12/2024, 14.00	6	5,1	Sunny	0,9				
26	11/12/2024, 15.00	4	3,1	Sunny	0,9				
27	11/12/2024, 16.00	2	2,2	Cloudy	-0,2				
28	12/12/2024, 08.00	3	3,2	Sunny	-0,2				
29	12/12/2024, 09.00	5	4,7	Sunny	0,3				
30	12/12/2024, 10.00	7	6,5	Sunny	0,5				
31	12/12/2024, 11.00	8	7,6	Cloudy	0,4				
32	12/12/2024, 12.00	7	6,7	Sunny	0,3				
33	12/12/2024, 13.00	7	5,2	Sunny	1,8				
34	12/12/2024, 14.00	6	5,5	Sunny	0,5				
35	12/12/2024, 15.00	4	3,6	Sunny	0,4				
36	12/12/2024, 16.00	2	2,5	Cloudy	-0,5				
37	13/12/2024, 08.00	3	3,2	Sunny	-0,2				
38	13/12/2024, 09.00	5	4,7	Sunny	0,3				
39	13/12/2024, 10.00	7	5,6	Sunny	1,4				
40	13/12/2024, 11.00	8	6,6	Cloudy	1,4				
41	13/12/2024, 12.00	7	6,7	Sunny	0,3				
42	13/12/2024, 13.00	7	5,3	Sunny	1,7				
43	13/12/2024, 14.00	6	5,5	Sunny	0,5				
44	13/12/2024, 15.00	4	3,6	Sunny	0,4				
	-5,12,2521,15.00		2,0	~ı	V, 1				

The test results show that the values obtained from the UV meter generally approach the reference data from the Uvindex.app application, with correction differences ranging from -0.5 to 1.8. In clear weather, the corrections tend to be positive, indicating that the UV meter shows slightly lower values than the reference. On the other hand, in cloudy weather, the correction variations are larger, including some negative values, such as on November 28, 2024, at 16:00 (-0.5) and

December 13, 2024, at 16:00 (-0.4). The highest UV intensity is consistently recorded between 11:00 and 13:00, when the sun is at its peak, while lower UV intensities are observed during the morning and evening.

This testing also shows that the UV sensor is highly sensitive to cloud cover conditions, causing significant data fluctuations, especially under cloudy conditions. In addition, external factors such as shading from the observer or other objects introduce noise, affecting the measurement results. As a result, the measurements at certain times become less stable. Nevertheless, the UV meter provides fairly consistent measurements under most conditions, with most corrections falling within the ± 1.5 range. Given the instrument's sensitivity to various environmental factors, caution is needed during operation to minimize noise influences and ensure that the data generated is more representative.

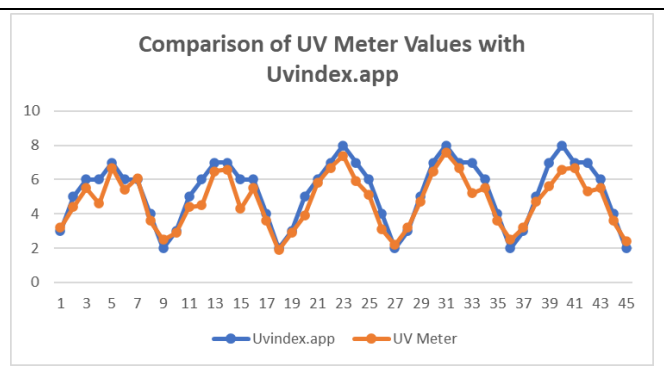


Fig. 18 Comparison Graph of UV Meter Reading and Data from uvindex.app Website

This figure compares the UV values from Uvindex.app (blue line) and the UV Meter (orange line) over a specific period. Both methods show a similar pattern, with UV peaks ranging from 8 to 9 and the lowest points approaching 2. Although the trend is consistent, there are slight differences at some points between the two measurements.

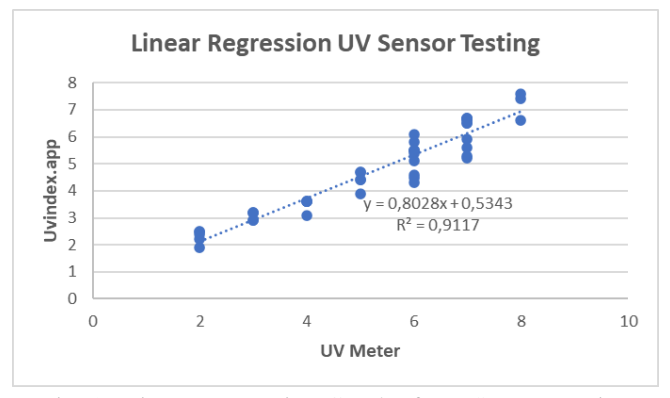


Fig. 19 Linear Regression Graph of UV Sensor Testing

This image presents a linear regression test between the UV values measured using a UV Meter (horizontal axis) and Uvindex.app (vertical axis). The pattern of the data points indicates A positive correlation between the two variables is demonstrated, further validated by the linear regression equation y = 0.8028x + 0.5343 and the coefficient of determination $R^2 = 0.9117$. The R^2 value, which is close to 1, indicates a strong correlation between the two methods, despite a slight deviation. Overall, these results suggest that the UV measurements obtained using Uvindex.app are consistent with those of the UV Meter, with only minor differences identifiable in the data.

3.3 Blynk Testing

The Blynk testing was conducted simultaneously with the UV Meter testing under direct sunlight exposure. The results showed that Blynk was able to display UV Meter data in real- time, including information on UV intensity categories, time, and UV reading graphs in line format. Thus, Blynk provides an informative and structured data visualization of UV to monitor changes in UV values directly.



Fig. 20 Blynk Desktop Display



Fig. 21 Blynk Android Display

In addition to being accessible via desktop, Blynk can also be used on Android devices by downloading the Blynk IoT app. This app allows users to access the same data by connecting it to their Blynk account, enabling flexible UV Meter monitoring across various devices.

4. CONCLUSION

The IoT-based UV index measuring device using the UVM- 30A sensor has been successfully designed and tested with satisfactory results. All components, such as the DS3231 RTC, 20x4 LCD, and data monitoring system via the Blynk platform, function as designed and support the optimal performance of the device. The IoT feature facilitates real-time remote data monitoring, while the integration of the solar tracker allows the UV sensor to efficiently receive sunlight, resulting in more accurate UV index measurements.

Test results show good measurement accuracy, with a comparison of the UV meter results against data from the uvindex.app website yielding a small relative error. However, the device is more sensitive to environmental factors, such as cloud cover and shading, which may unintentionally block the sensor. With sufficient flexibility, performance, and accuracy, this device is an effective solution for real-time and accurate UV index measurements.

REFERENCE

- [1] W. Li and S. Fan, "Nanophotonic control of thermal radiation for energy applications [Invited]," Opt Express, vol. 26, no. 12, p. 15995, Jun. 2018, doi: 10.1364/oe.26.015995.
- [2] A. Dwivedi, A. K. Tripathi, J. Singh, and M. K. Pal, "Ultraviolet radiation (UVR): An introduction," in Photocarcinogenesis and Photoprotection, Springer Singapore, 2018, pp. 1–8. doi: 10.1007/978-981-10-5493-8_1.
- [3] E. C. Turner, J. Manners, C. J. Morcrette, J. B. O'Hagan, and A. R.
 D. Smedley, "Toward a New UV Index Diagnostic in the Met Office's Forecast Model," J Adv Model Earth Syst, vol. 9, no. 7, pp. 2654–2671, Nov. 2017, doi: 10.1002/2017MS001050.
- [4] J. C. S. Yam and A. K. H. Kwok, "Ultraviolet light and ocular diseases," 2014, Kluwer Academic Publishers. doi: 10.1007/s10792-013-9791-x.
- [5] R. M. Lucas et al., "Human health in relation to exposure to solar ultraviolet radiation under changing stratospheric ozone and climate," Photochemical and Photobiological Sciences, vol. 18, no. 3, pp. 641–680, 2019, doi: 10.1039/C8PP90060D.
- [6] C. J. Heckman, K. Liang, and M. Riley, "Awareness, understanding, use, and impact of the UV index: A systematic review of over two decades of international research," Jun. 01, 2019, Academic Press Inc. doi: 10.1016/j.ypmed.2019.03.004.
- [7] T. Furuhashi, K. Torii, K. Ikumi, H. Kato, E. Nishida, and A. Morita, "Ultraviolet A1 phototherapy for the treatment of localized scleroderma," Journal of Dermatology, vol. 47, no. 7, pp. 792–795, Jul. 2020, doi: 10.1111/1346-8138.15368.
- [8] D. R. Roshan, M. Koc, A. Abdallah, L. Martin-Pomares, R. Isaifan, and C. Fountoukis, "UV index forecasting under the influence of desert dust: Evaluation against surface and satellite-retrieved data," Atmosphere (Basel), vol. 11, no. 1, 2020, doi: 10.3390/ATMOS11010096.
- [9] A. C. G. B. Leal, M. P. Corrêa, M. F. Holick, E. V. Melo, and M. Lazaretti-Castro, "Sun-induced production of vitamin D3 throughout 1 year in tropical and subtropical regions: relationship with latitude,

- cloudiness, UV-B exposure and solar zenith angle," Photochemical and Photobiological Sciences, vol. 20, no. 2, pp. 265–274, Feb. 2021, doi: 10.1007/s43630-021-00015-z.
- [10] P. Gies, E. Van Deventer, A. C. Green, C. Sinclair, and R. Tinker, "Review of the Global Solar UV Index 2015 Workshop Report," Jan. 01, 2018, Lippincott Williams and Wilkins. doi: 10.1097/HP.0000000000000742.
- [11] N. C. Delic, J. G. Lyons, N. Di Girolamo, and G. M. Halliday, "Damaging Effects of Ultraviolet Radiation on the Cornea," Jul. 01, 2017, Blackwell Publishing Inc. doi: 10.1111/php.12686.
- [12] N. A. Pramono, F. I. Sofyan, B. A. Purwandani, and O. Ghaisyani, "Application of ESP32 as a Media for Learning Ozone Damage in the Form of IoT-Based Ultraviolet Index Readers."
- [13] E. Lönnqvist et al., "Wearable UV Meter An EPS@ISEP 2017 Project," in Advances in Intelligent Systems and Computing, Springer Verlag, 2018, pp. 896–907. doi: 10.1007/978-3-319-73210-7_102.
- [14] M. Blumthaler, "UV monitoring for public health," Int J Environ Res Public Health, vol. 15, no. 8, Aug. 2018, doi: 10.3390/ijerph15081723.
- [15] E. Ervianto et al., "Assessing the Efficacy of the UV Index in Predicting Surface UV Radiation: A Comprehensive Analysis Using Statistical and Machine Learning Methods," Indonesian Review of Physics, vol. 6, no. 2, pp. 99–121, Dec. 2023, doi: 10.12928/irip.v6i2.8216.
- [16] R. Duarte Almeida, R. Barreto, E. Souto, and J. Cabral Leite, "IoT System for Ultraviolet Ray Index Monitoring," Int J Innov Educ Res, vol. 7, no. 12, pp. 409–420, Dec. 2019, doi: 10.31686/ijier.vol7.iss12.2087.
- [17] M. N. A. Mohd Said, S. A. Jumaat, and C. R. A. Jawa, "Dual axis solar tracker with iot monitoring system using arduino," International Journal of Power Electronics and Drive Systems, vol. 11, no. 1, pp. 451–458, Mar. 2020, doi: 10.11591/ijpeds.v11.i1.pp451-458.
- [18] C. Jamroen, C. Fongkerd, W. Krongpha, P. Komkum, A. Pirayawaraporn, and N. Chindakham, "A novel UV sensor-based dual-axis solar tracking system: Implementation and performance analysis," Appl Energy, vol. 299, Oct. 2021, doi: 10.1016/j.apenergy.2021.117295.
- [19] G. Tejaleksono, D. Notosudjono, A. R. Machdi, F. Adzikri, and A. U. Rahayu, "PROTOTYPE OF CO, CO 2, UV LIGHT, TEMPERATURE, AND HUMIDITY DETECTION DEVICE BASED ON IOT AND SOLAR CELLS," 2024.
- [20] U. V Iac, "INTERSUN PROGRAMME 7 International Advisory Committee Meeting," 2018